CROSS SECTIONS OF THE ^{144}Sm(n,α)^{141}Nd REACTION AT 5.5 AND 6.5 MeV

Yu.M. Gledenov[1], M.V. Sedysheva[1], L. Krupa[2,3], E. Sansarbayar[1], G. Khuukhenkhuu[4], Haoyu Jiang[5], Huaiyong Bai[5], Yi Lu[5], Zengqi Cui[5], Jinxiang Chen[5], Guohui Zhang[5]

[1]*Frank Laboratory of Neutron Physics, Joint Institute for Nuclear Research, Dubna 141980, Russia*
[2]*Flerov Laboratory of Nuclear Reactions, Joint Institute for Nuclear Research, Dubna 141980*
[3]*Institute of Experimental and Applied Physics, Czech Technical University in Prague, Horska*
[4]*Nuclear Research Centre, National University of Mongolia, Ulaanbaatar, Mongolia*
[5]*State Key Laboratory of Nuclear Physics and Technology, Institute of Heavy Ion Physics, Peking University, Beijing 100871, China*

ABSTRACT

The ^{144}Sm(n,α)^{141}Nd cross sections were measured at E_n = 5.5 and 6.5 MeV. The experiments were performed at the 4.5 MV Van de Graaff Accelerator of Peking University. A twin-gridded ionization chamber was used as the detector, and back-to-back $^{144}Sm_2O_3$ samples were mounted on its common cathode. The mono-energetic neutrons were generated using energetic deuteron beam from the accelerator to bombard a deuterium gas target. The relative neutron flux was monitored using a BF_3 long counter. The absolute neutron flux was calibrated using a ^{238}U standard sample. The present results are compared with existing measurements and evaluations.

I. INTRODUCTION

^{144}Sm, a stable isotope of samarium (natural abundance 3.08%), is the fission product in nuclear reactors. The study of ^{144}Sm(n,α)^{141}Nd reaction is important in nuclear engineering applications. Besides, measurements of this cross section could enhance our understanding in nuclear physics. For example, in nuclear astrophysics, the (n,α) cross sections of samarium could be used in the calculations of reaction rates which are significant in the analysis of explosive nucleosynthesis [1]. However, the measurements are quite scanty for this reaction. For neutron energies from 4 to 7 MeV, there is no measurement except our results in 2016 because of the small cross section of this reaction and the low intensity of the neutron flux [2]. For other neutron energy region, only three measurements exist around 14 MeV, and there are three-times differences among them [3-5]. Thus, the ^{144}Sm(n,α)^{141}Nd reaction cross section differs by more than one orders of magnitude among different evaluated nuclear data libraries [6]. So, accurate measurements are demanded to clarify exciting discrepancies among different libraries and address application needs.

For samarium isotopes, we have measured the cross sections of the ^{144}Sm(n,α)^{141}Nd at E_n = 4.0, 5.0 and 6.0 MeV [2], the ^{147}Sm(n,α)^{144}Nd reaction at E_n = 5.0 and 6.0 MeV [7], and the ^{149}Sm(n,α)^{146}Nd reaction at E_n = 4.5, 5.0, 5.5, 6.0 and 6.5 MeV [8,9]. In the present work, we measured the ^{144}Sm(n,α)^{141}Nd reactions at E_n = 5.5 and 6.5 MeV.

II. DETAILS OF EXPERIMENTS

The experiments were performed at the 4.5-MV Van de Graaff accelerator of Peking University, China. The experimental apparatus, which is shown in Fig.1, consists of three main parts: the neutron source, the charged particle detector (with samples inside) and the neutron flux monitor.

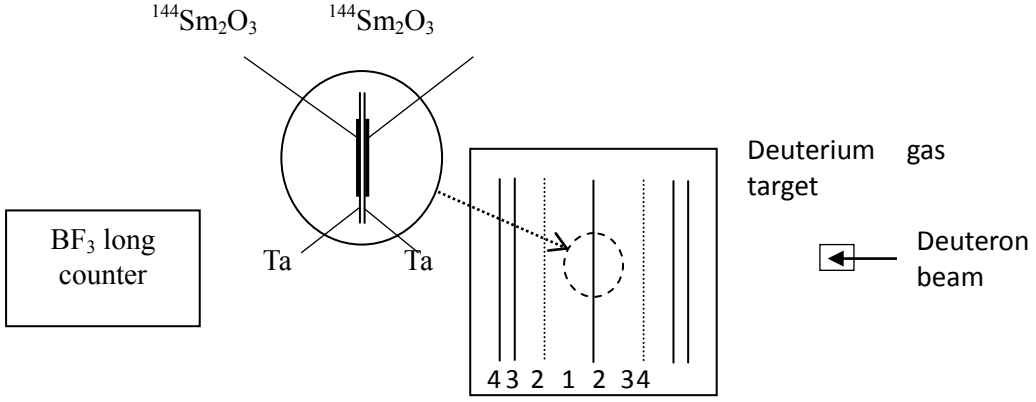

1– Cathode; 2– Grid; 3– Anode; 4– Shield

Fig. 1. Experimental setup.

The mono-energetic neutrons were generated using energetic deuteron beam from the accelerator to bombard a deuterium gas target. For neutron energies of 5.5 and 6.5 MeV, the corresponding neutron energy spreads (1σ) were 0.14 and 0.10 MeV, respectively [9]. The beam current was about 2.0 μA throughout the measurement.

The α-particle detector is a twin gridded ionization chamber (GIC) with a common cathode, and its structure can be found in Ref. [10]. The distance from the cathode to the grid was 61 mm, from grid to anode was 15 mm, and from the position of samples to the near end of the gas target cell was 15.25 cm. Working gas of the GIC was Kr +2.83% CO_2, and the pressure is 2.02 atm for the α-particles to be stopped before reaching the grids. High voltages applied on the cathodes and anodes were -2600 V and 1300 V (the grids electrodes were grounded) which allowed complete collection of electrons from the ionization tracks.

A sample changer was set at the common cathode of the ionization chamber with five sample positions, and back-to-back double samples can be placed at each of them. The sample positions could be changed without opening the GIC. Each $^{144}Sm_2O_3$ sample was prepared on the 0.1mm thick tantalum backing. Two back-to-back $^{144}Sm_2O_3$ samples were mounted on the common cathode so that forward ($0^\circ \sim 90^\circ$) and backward ($90^\circ \sim 180^\circ$) emitted α-particles can be detected simultaneously. Data of the samples are listed in Table 1, and the number of ^{144}Sm atoms in the samples was determined by weighing the samples. Besides, two back-to-back tantalum films 0.1 mm in thickness were mounted on another sample position for background measurements. In addition, two compound α-sources were back-to-back placed at one of the sample positions for energy calibration and adjustment of the data acquisition system.

TABLE I. Description of the samples.

Samples	Material	Isotopic enrichment(%)	Thickness (μg/cm^2)	Diameter (mm)
^{144}Sm	$^{144}Sm_2O_3$	95.0	4084[a] and 3177[b]	44.0[a] and 44.0[b]
^{238}U	$^{238}U_3O_8$	99.999	604.84	45.0

[a] Forward sample. [b] Backward sample.

To determine the absolute neutron flux, a ^{238}U film sample described in Table I was placed at the forward direction of the other position of the sample changer in the GIC.

In order to monitor the relative neutron flux during measurements, a BF_3 long counter was used for all runs. The axis of the counter was along the normal line of the electrodes of the ionization chamber as well as the 0° direction of the deuteron beam line. The distance from the BF_3 long counter to the GIC was approximately 3.0 m.

Cathode-anode coincident two-dimensional spectra of the gridded ionization chamber were recorded for both forward and backward charged particles. The data-acquisition system was described in Ref. [11]. For each neutron energy point, the experimental process was as follows: 1) compound α source measurement for energy calibration, 2) foreground measurement for α events of the ^{144}Sm(n,α)^{141}Nd reaction, 3) background measurement with tantalum foils, 4) ^{238}U fission events measurement for absolute neutron flux calibration, and 5) α source measurement again. However, because the Q value (7.874 MeV) of the ^{144}Sm(n,α)^{141}Nd reaction is rather large, and we found the background was quite weak when we measured it at E_n = 5.5 MeV, we did not measure the background at the 6.5 MeV neutron energy point.

At the 5.5 MeV neutron energy point, the beam durations for foreground, background and absolute neutron flux calibration were about 30.5, 15.0 and 3.0 h, respectively. And at the 6.5 MeV neutron energy point, the beam durations for foreground and absolute neutron flux calibration were about 17.0 and 3.5 h, respectively. So, the total beam time for the two neutron energies was about 69.0 h.

The cross section σ of the ^{144}Sm(n,α)^{141}Nd reaction can be calculated from the following equations:

$$\sigma = \sigma_f \cdot \frac{N_\alpha \cdot \varepsilon_f \cdot N_{238\mathrm{U}} \cdot N_{\mathrm{BF_3}f}}{N_f \cdot \varepsilon_\alpha \cdot N_{\mathrm{samp}} \cdot N_{\mathrm{BF_3fore}}} \tag{1}$$

$$N_\alpha = N_{\alpha\mathrm{fore}} - \frac{N_{\mathrm{BF_3fore}}}{N_{\mathrm{BF_3back}}} N_{\alpha\mathrm{back}} \tag{2}$$

Where σ_f is the standard cross section of the ^{238}U(n, f) reaction taken from IAEA Neutron Cross-section References (2015) [12]. The N_α is α counts above the energy threshold (after background subtraction) from the ^{144}Sm(n,α)^{141}Nd reaction. N_f is the fission counts from the ^{238}U(n, f) reaction above the energy threshold. ε_α and ε_f are the detection efficiency for α-particles and fission fragments, respectively, and they were calculated through the simulated anode spectra. The calculation details will be discussed in the next section. $N_{238\mathrm{U}}$ and N_{samp} are the numbers of ^{238}U and ^{144}Sm nuclei in the samples, respectively. $N_{\mathrm{BF_3}f}$, $N_{\mathrm{BF_3fore}}$ and $N_{\mathrm{BF_3back}}$ are the counts of the neutron flux monitor (BF_3 counter) for ^{238}U fission, ^{144}Sm(n,α)^{141}Nd foreground measurements and background measurements, respectively. $N_{\alpha\mathrm{fore}}$ and $N_{\alpha\mathrm{back}}$ are the α event counts of foreground and background measurements of ^{144}Sm(n,α)^{141}Nd reaction, respectively. According to Eqs. (1) and (2), forward and backward

^{144}Sm(n,α)^{141}Nd cross sections could be calculated. Subsequently, total (n,α) cross section could be acquired by adding the forward cross section and backward cross section together. And forward/backward ratios could be obtained through the division of the forward cross section and backward cross section.

III. DATA PROCESSING AND RESULTS

The data processing methods are similar for the measurements at the two neutron energies. Take the forward direction data of the ^{144}Sm(n,α)^{141}Nd reaction at 5.5 MeV neutron energy as an example, the data are processed as follows.

First, the two-dimensional spectrum of the compound α-sources was used for energy calibration, and the 0° and the 90° curves determination. Fig.2 shows the valid-event-area of α events which should locate between the 0° and 90° curves.

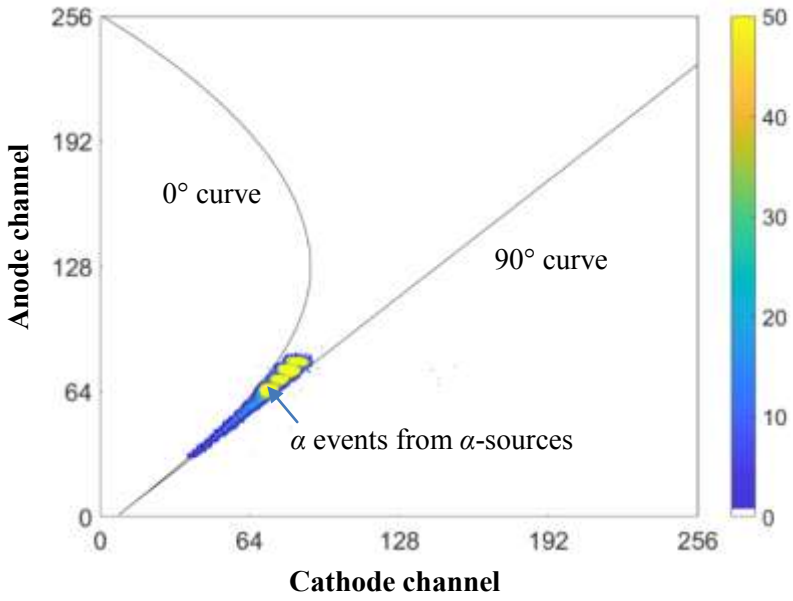

Fig. 2. Two-dimensional spectrum of the compound α sources of the forward direction.

Second, the two-dimensional spectrum of the ^{144}Sm(n,α)^{141}Nd reaction was analyzed. Fig.3 shows the cathode-anode two-dimensional spectrum after background subtraction at the 5.5 MeV neutron energy point in the forward direction. The effective α events from the ^{144}Sm(n, α)^{141}Nd reaction could be picked through their relatively higher energies comparing with the background events.

Third, the detection efficiency (ε_α) of α-particles was determined after projecting the two-dimensional spectrum to the anode channel. The detection efficiency was related to two aspects: 1) the number of events with amplitudes below threshold (the threshold correction), and 2) the number of events absorbed in the samples (the self-absorption correction) [13]. Both of the corrections could be calculated using the simulation of the anode spectra. For the spectrum simulation, the stopping power of α-particles in the samples was calculated using SRIM-2013 [14], and the angular and energy distributions of α-particles from the ^{144}Sm(n,α)^{141}Nd reaction were calculated by Talys-1.9 [15]. To obtain better results, we adjust two parameters from default values. The microscopic level densities from Goriely's tables (ldmodel 4 in Talys-1.9) were used, and the geometry radius parameter r_V of the optical model

were adjusted from 1 (the default) to 1.012 for α particle. The calculated total (n,α) cross sections are closed to the measured values, but the calculated forward/backward ratios could not agree with the measured results. The measured forward/backward ratios were used in obtaining the simulated anode spectra. As an example, the simulated anode spectrum (purple line) compared with that from measurement (blue curve) at E_n = 5.5 MeV for the forward direction is shown in Fig.4.

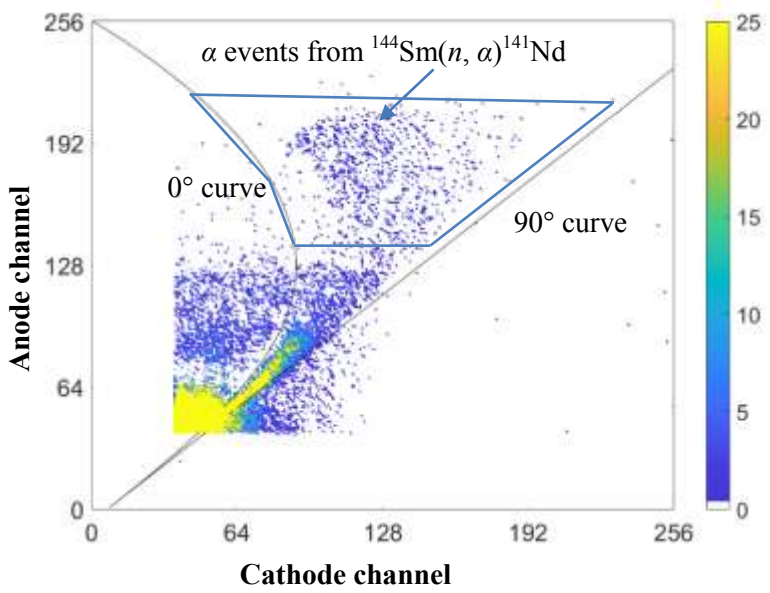

Fig. 3. Two-dimensional spectrum of the ^{144}Sm(n,α)^{141}Nd reaction at E_n = 5.5 MeV in the forward direction.

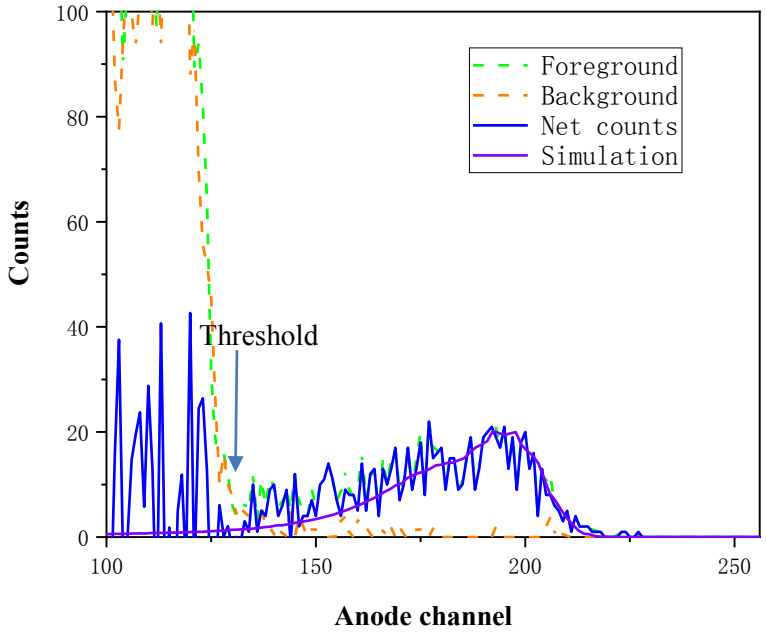

Fig. 4. Anode spectrum of the ^{144}Sm(n,α)^{141}Nd reaction at E_n = 5.5 MeV for the forward direction.

The corrected α counts are obtained through the division of α counts above threshold (N_α) and the detection efficiency (ε_α), which were calculated through the simulated anode spectra. The detection efficiency (ε_α) is related to the position of threshold, and we would give the error of ε_α by changing the position of threshold. At 5.5 MeV neutron energy, the detection efficiency (ε_α) of the ^{144}Sm(n, α)^{141}Nd reaction is 87.34% for the forward direction and 87.15% for the backward direction, and at 6.5 MeV neutron energy, the detection efficiency (ε_α) is 84.20% for the forward direction and 83.61% for the backward direction.

Fourth, the absolute neutron flux was determined by the ^{238}U(n, f) reaction fission counts. The anode spectrum of the fission fragments at 5.5 MeV neutron energy is shown in Fig.5 with blue line. To determine the detection efficiency (ε_f) of fission fragments, the Monte Carlo simulation was used for threshold and self-absorption corrections. The stopping power of fission fragments in the samples was calculated by SRIM [14] and the fission production yield was calculated by GEF code [16]. Details of simulation can be found in Ref. [17]. The red curve in Fig. 5 shows the simulated result for the fission fragments. Through the simulated anode spectra and the threshold, the detection efficiency (ε_f) could be calculated. The detection efficiency (ε_f) of the fission fragments is 70.55% for E_n = 5.5 MeV and 69.98% for E_n = 6.5 MeV, respectively.

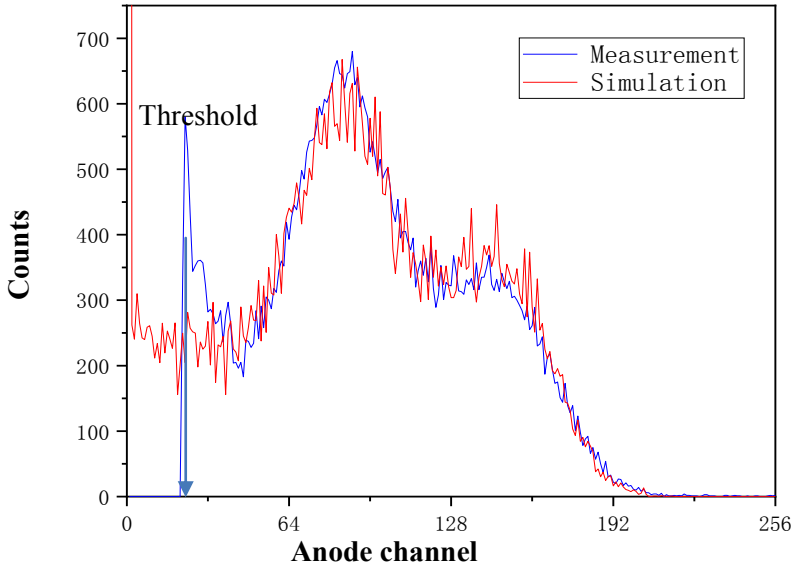

Fig. 5. Anode spectrum of the ^{238}U fission fragments at E_n = 5.5 MeV.

According to Eqs. (1) and (2), forward and backward ^{144}Sm(n, α)^{141}Nd cross sections were calculated. Subsequently, total (n, α) cross sections and forward/backward ratios in the laboratory reference system were calculated, and the results are listed in Table III.

TABLE III. Measured ^{144}Sm(n, α)^{141}Nd cross sections and forward/backward ratios (in the laboratory reference system) compared with Talys-1.9 calculations (ldmodel 4, 1.012r_V)

E_n(MeV)	$\sigma_{(n,\alpha)}$ (mb)		Forward/backward ratio	
	Measurement	Calculation	Measurement	Calculation
5.5	0.19±0.02	0.21	2.04±0.36	1.02
6.5	0.41±0.06	0.40	2.70±0.79	1.02

For the total ^{144}Sm(n,α)^{141}Nd cross sections, good agreements are achieved between present measurements and theoretical calculations using Talys-1.9. However, for the forward/backward ratios, the calculated results could not reproduce the experimental data. At the MeV region, ^{144}Sm(n,α)^{141}Nd cross sections have large forward/backward ratios. For samarium isotopes, the forward/backward ratios are generally bigger than those from the model calculations, and this phenomena were also confirmed by other measurements [2, 7–9]. The contribution of non-statistical effects might lead to these deviations between the measured results and the model calculations.

The sources of uncertainty and their magnitudes are listed in Table IV. The uncertainty was calculated by the error propagation formula. Major source of uncertainty was the detection efficiency of α-particles for both E_n = 5.5 and 6.5 MeV. Around the neutron energy of 6.5 MeV, the cross sections of the ^{238}U(n, f) reaction change rapidly as the neutron energy increases, and it would lead to big uncertainty of fission counts in the determination of the absolute neutron flux. So, the neutron energy spreads would be another major source of uncertainty at E_n = 6.5 MeV.

At the 6.5 MeV neutron energy point, because we did not measure the background, the background of E_n = 5.5 MeV was used for the subtraction. Due to the difference of neutron energy, the error caused by background uncertainty was considered. We increased the background counts of E_n = 5.5 MeV by 100%, and recalculated the ^{144}Sm(n, α)^{141}Nd reaction cross section at 6.5 MeV neutron energy point. The error was obtained by comparing the new cross section with the original one.

TABLE IV. Sources of uncertainty and their magnitudes.

Sources of uncertainty	Magnitude (%)	
	5.5 MeV	6.5 MeV
Statistical error of α-particles (N_α)	3.45[a] 5.60[b]	3.49[a] 6.50[b]
Valid-event-area of α-sources events (N_α)	0.47[a] 0.70[b]	0.15[a] 1.03[b]
Detection efficiency of α-particles (ε_α)	6.16[a] 11.82[b]	5.13[a] 9.49[b]
Background reduction ($N_{\alpha\mathrm{back}}$)	1.41[a] 3.68[b]	0.87[a] 3.88[b]
Background uncertainty ($N_{\alpha\mathrm{back}}$)	Only for 6.5 MeV	3.09[a] 17.82[b]
Neutron energy spreads (N_f)	0.80	6.87
Statistical error of fission events (N_f)	0.45	0.54
Detection efficiency for fission fragment (ε_f)	5.11	5.03
Numbers of ^{238}U nucleus ($N_{238\mathrm{U}}$)	0.45	0.45
^{238}U (n, f) cross sections (σ_f)	0.70	0.70
Normalization of the BF_3 counts ($N_{\mathrm{BF_3}}$)	3.30	9.65
Numbers of ^{144}Sm nucleus (N_{samp})	1.00	1.00
Total	9.1	15.1

[a] For the forward results of the ^{144}Sm(n, α)^{141}Nd reaction

[b] For the backward results of the ^{144}Sm(n, α)^{141}Nd reaction

(The symbols in the parentheses refer to the quantities in Eqs. (1) and (2), $N_{\mathrm{BF_3}}$ refers to the counts of the BF_3 counter.)

Results of the present experiments are compared with existing measurements, evaluations, and Talys-1.9 calculations (ldmodel 4, $1.012r_V$) as shown in Fig. 6. In both magnitude and tendency, there are order of magnitude differences among different evaluation libraries in the MeV region. Our experiment results are closer to the data of TENDL-2015 libraries [18]. The Talys-1.9 calculations agree with our present measurements as well as the Alford's and Luo's results in the 14 MeV region. However, the present experiment results are higher than our measurements in 2016, therefore further measurements in the MeV region are necessary to clarify the discrepancies among different libraries and experiments.

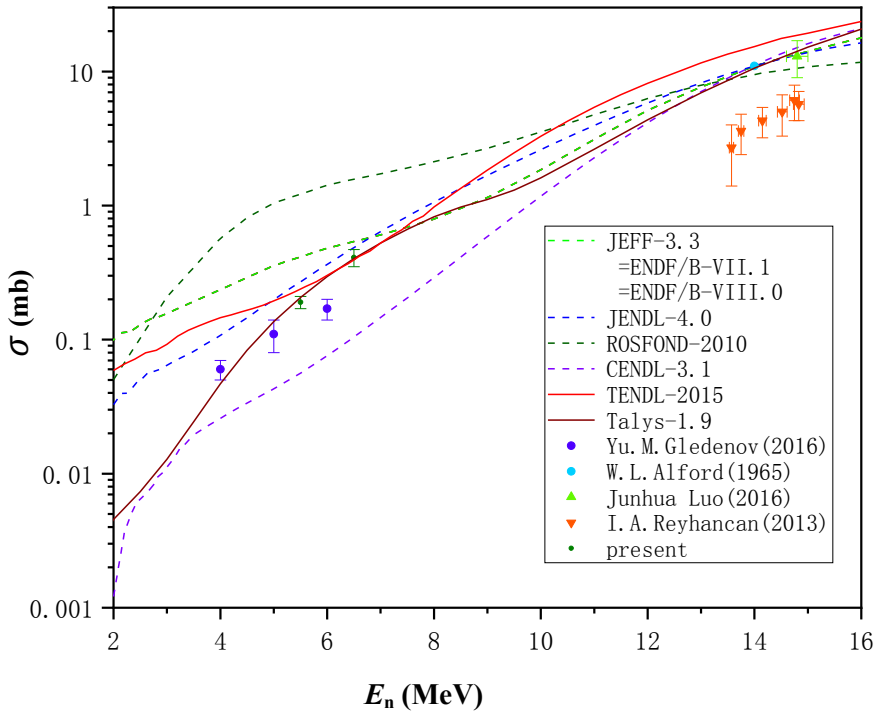

Fig. 6. Present cross sections of the ^{144}Sm(n,α)^{141}Nd reaction compared with existing measurements, evaluations and Talys-1.9 calculations (ldmodel 4, $1.012r_V$).

IV. CONCLUSIONS

In the present work, cross sections of the ^{144}Sm(n,α)^{141}Nd reaction were measured at 5.5 and 6.5 MeV neutron energy points. There are very large discrepancies among different evaluation libraries, and our results are closer to the data of TENDL-2015 library. Theoretical analyses using Talys-1.9 code was performed, and agreement was achieved between present measurements and calculations. The present results are higher than our measurements in 2016, and further experiments in the MeV region are necessary to clarify the discrepancies among different libraries and measurements.

ACKNOWLEDGEMENTS

The authors are indebted to the operation crew of the 4.5-MV Van de Graaff accelerator of Peking University. The present work was financially supported by the National Natural Science Foundation of China (11775006 and 11475007), China Nuclear Data Center and the Science and Technology on Nuclear Data Laboratory.

REFERENCES

[1] Yu.M. Gledenov, P.E. Koehler, J. Andrzejewski, and K.H. Guber, Phys. Rev. C **62**, 042801(R) (2000).

[2] Gledenov Yury, Zhang Guohui, Gonchigdorj Khuukhenkhuu, Sedysheva Milana, Krupa Lubos, Enkhbold Sansarbayar, Chuprakov Igor, Wang Zhimin, Fan Xiao, Zhang Luyu, and Bai Huaiyong, EPJ Web of Conferences **146**, 11033 (2017).

[3] I. A. Reyhancan, A. Durusoy, Nuclear Science and Engineering, **174**, 202 (2013).

[4] W.L. Alford, R.D. Koehler, Bulletin of the American Physical Society, **10**, 260 (1965).

[5] Luo J., Wu C., Jiang L., Long H., Radiochimica Acta, **104**, 523 (2016).

[6] ENDF: Evaluated Nuclear Data File, Database Version of 2018-02-13, https://www-nds.iaea.org/exfor/endf.htm.

[7] Yu.M. Gledenov, M.V. Sedysheva, V.A. Stolupin, Guohui Zhang, Jiaguo Zhang, Hao Wu, Jiaming Liu, Jinxiang Chen, G. Khuukhenkhuu, P.E. Koehler, and P.J. Szalanski , Physical Review C, **80**, 044602 (2009).

[8] Yu.M. Gledenov, Guohui Zhang, G. Khuukhenkhuu, M.V. Sedysheva, P.J. Szalanski , P.E. Koehler, Jiaming Liu, Hao Wu, Xiang Liu, and Jinxiang Chen, Physical Review C, **82**, 014601 (2010).

[9] Guohui Zhang, Yu.M. Gledenov, G. Khuukhenkhuu, M.V. Sedysheva, P.J. Szalanski, P.E. Koehler, Yu.N. Voronov, J. Liu, X. Liu, J. Han, and J. Chen, Physical Review Letters, **107**, 252502 (2011).

[10] X. Zhang, Z. Chen, Y. Chen, J. Yuan, G. Tang, G. Zhang, J. Chen, Y. M. Gledenov, G. Khuukhenkhuu, and M. Sedysheva, Physical Review C **61**, 054607 (2000).

[11] Guohui Zhang, Hao Wu, Jiaguo Zhang, Jiaming Liu, Yu.M. Gledenov, M.V. Sedysheva, G. Khuukhenkhuu, and P.J. Szalanski, Eur. Phys. J. A, **43**, 1 (2010).

[12] Pronyaev V., Simakov S., Marcinkevicius B., University of Leeds, **158**, 80 (2015).

[13] Yu.M. Gledenov, M.V. Sedysheva, V.A. Stolupin, Guohui Zhang, Jinhua Han, Zhimin Wang, Xiao Fan, Xiang Liu, Jinxiang Chen, G. Khuukhenkhuu, and P.J. Szalanski , Physical Review C, **89**, 064607 (2014).

[14] J.F. Ziegler, SRIM-2013, http://www.srim.org/#SRIM.

[15] A.J. Koning, S. Hilaire, and M.C. Duijvestijn, TALYS-1.9, http://www.talys.eu/.

[16] K.-H. Schmidt, B. Jurado, C. Amouroux and C. Schmitt, Nuclear Data Sheets **131**, 107 (2016).

[17] Haiyong Bai, Haoyu Jiang, Yi Lu, Zengqi Cui, Jinxiang Chen, Guohui Zhang, "Determined of the ^{238}U nucleus number and simulation of neutron induced fission energy spectrum" (to be published).

[18] A.J. Koning, D. Rochman, J. Kopecky, J. Ch. Sublet, E. Bauge, S. Hilaire, P. Romain, B. Morillon, H. Duarte, S. van der Marck, S. Pomp, H. Sjostrand, R. Forrest, H. Henriksson, O. Cabellos, S. Goriely J. Leppanen, H. Leeb, A. Plompen and R. Mills, "TENDL-2015: TALYS-based evaluated nuclear data library", https://tendl.web.psi.ch/tendl_2015/tendl2015.html.